Chemical Engineering Journal 109 (2005) 133–139

Chemical Engineering Journal

www.elsevier.com/locate/cej

Effect of preparation methods on the structure and redox behavior of platinum–ceria–zirconia catalysts

Xiaodong Wu *, Jun Fan, Rui Ran, Duan Weng

Department of Materials Science and Engineering, Tsinghua University, Beijing 100084, China

Received 1 September 2004; received in revised form 22 March 2005; accepted 11 April 2005

Abstract

Platinum was introduced into ceria–zirconia solid solutions to form nominal $Ce_{0.66}Zr_{0.32}Pt_{0.02}O_2$ solid solutions by sol–gel. It was found that, through sol–gel method, the Pt ions could be inserted into the ceria lattice according to the results of XRD, XPS and TPR analyses. This brought about a different synergistic effect between the Pt and Ce components in $Ce_{0.66}Zr_{0.32}Pt_{0.02}O_2$ compared with the $Pt/Ce_{0.67}Zr_{0.33}O_2$ system prepared by traditional impregnation, such as increased the oxygen mobility in ceria–zirconia solid solutions and improved the stability of metallic state for platinum at high temperature. The lower surface Pt content leads to a worse three-way catalytic activity over the Pt-doped sample at low temperature. However, it features a better thermal stability after aging at 950 °C for 20 h, implying a self-generation mechanism of noble metals. This, in return, provides this material with a potential to be used in eliminating pollutants from auto exhaust.

Keywords: Three-way catalysts; Platinum; Ceria–zirconia solid solutions; Synthesis

1. Introduction

Three-way catalysts (TWCs) have been widely used to control the automotive exhaust pollution. Classical TWCs consist of noble metals (Rh, Pt and/or Pd) supported on high-surface-area alumina. In order to obtain high conversion rates for CO, HC and NO, the air/fuel (A/F) ratio oscillations that occur in automotive exhaust under normal operating conditions should be buffered. Therefore, ceria has been pervasively used as an oxygen storage material. Associated to the redox couple of Ce^{4+}/Ce^{3+}, this material can provide oxygen required by oxidation of CO and HC when the engine is running under a fuel-rich condition, and absorb oxygen to ensure the reduction of NO when the condition turns to fuel-lean. Thus, a ceria-containing catalyst receiving a rapidly cycled exhaust gas feedstream that averages out as stoichiometric over time can function as efficiently as if it receives a steady state stoichiometric feed.

The more stringent emission control emissions require the TWCs to be installed closer to the engine. Here the temperature of the catalyst can be as high as 1000–1100 °C, demanding a good thermal stability. The pure CeO_2 tends to sinter above 800 °C, hereby decreasing and even losing the oxygen storage capacity (OSC). One approach to achieve more thermal stable materials is to modify ceria by doping it with other oxides, such as La_2O_3 and Ga_2O_3 [1,2]. Most recently ZrO_2 has been recognized as perhaps the most effective dopant for ceria [3–8]. Compared to pure ceria, inserting ZrO_2 into the ceria lattice to form ceria–zirconia solid solutions has improved the thermal stability and oxygen storage capacity. Whereas the OSC of ceria depends directly on its surface area, ceria–zirconia solid solutions are able to maintain high OSC despite severe sintering [9]. This property is believed to be related to the displacement of oxygen sublattice around zirconium, leading to higher oxygen mobility and easier bulk reduction of the solid solutions [10,11].

Usually, noble metals are impregnated on pure ceria or ceria–zirconia solid solutions with alumina as carrier to form TWCs. Many researches focus on the interaction between

* Corresponding author. Tel.: +86 10 62792375; fax: +86 10 62772726.
E-mail address: wuxiaodong@tsinghua.edu.cn (X. Wu).

1385-8947/$ – see front matter © 2005 Elsevier B.V. All rights reserved.
doi:10.1016/j.cej.2005.04.003

noble metals and ceria–zirconia solid solutions [12–14]. For example, Kenevey et al. [12] found noble metal assisted in the demixing process of $Ce_{0.50}Zr_{0.50}O_2$ by enhancing ionic mobility and promoting the nucleation of the new phases of $Ce_{0.18}Zr_{0.82}O_2$ and $Ce_{0.80}Zr_{0.20}O_2$. However, no effect of noble metal was observed for the $Ce_{0.68}Zr_{0.32}O_2$ system. This strongly suggested that there existed a particular interaction between noble metals and the support oxides which was dependent on the crystal structure assumed by the metal oxides. Bozo et al. [13] suggested that electron transfer from the oxide to the noble metal resulted in a lowering of the effective activation energy for the formation of oxygen vacancies. Thus, the presence of noble metal might enhance the number of oxygen vacancies and improve oxygen activation and mobility, hereby improving the catalytic activity. Fernández-García et al. [14] reported that the interaction between noble metals and ceria–ceira–zirconia solid solutions primarily promoted the activation of molecules such as NO and O_2 through a route involving anion vacancies on the lanthanide oxide but also changed drastically the noble metal response to the reaction atmosphere.

On the other hand, the interaction between noble metals and ceria–zirconia solid solutions has been scarcely studied in the integrated systems. Liu et al. [15] prepared the 17 wt.% $Pd/Ce_{0.8}Zr_{0.2}O_2$ catalyst by precipitation of the appropriate amounts of $Ce(NO_3)_3$, $ZrO(NO_3)_2$ and $Pd(NO_3)_2$ in aqueous solution using NaOH as the precipitating agent. The results of XRD and TEM analysis showed that partial Pd^{2+} ions entered into ceria–zirconia solid solutions. This catalyst showed a much higher conversion 51.2% for methanol decomposition to synthesis gas at 200 °C than 17.2% over the $Pd/Ce_{0.8}Zr_{0.2}O_2$ by impregnation. The authors attributed it to the fact that the coprecipitation catalyst possessed many small Pd particles. Primavera et al. [16] compared Pd–Ce–Zr–O mixed oxides prepared by coprecipitation to a $Pd/Ce_{0.8}Zr_{0.2}O_2$ catalyst in which the palladium was deposited on the performed support. This study focused on the effect of the calcination temperature on the activity in methane combustion. The supported catalysts behave better at low temperature, as expected from their higher surface Pd content. However, the drop in activity in high temperature, due to the decomposition of PdO, is less important with the Pd-containing mixed oxides, presumably because the palladium is stabilized in an oxidized form.

The aim of the present work was to investigate the effect of preparation methods on the structure and redox behavior of the Pt–Ce–Zr–O systems. Pt-doped ceria–zirconia solid solutions ($Ce_{0.66}Zr_{0.32}Pt_{0.02}O_2$) were synthesized by sol–gel. The equal quantity of Pt was impregnated on the surface of $Ce_{0.67}Zr_{0.33}O_2$ as a Pt-loaded sample. The samples were characterized by XRD, BET, TPR and XPS analyses, as well as the catalytic activity evaluation. We especially tried to explain the variations of the behaviors for these two catalysts from a viewpoint of the interaction between platinum and ceria–zirconia solid solutions.

2. Experimental

2.1. Catalyst preparation

$Ce_{0.67}Zr_{0.33}O_2$ was synthesized by citric-aided sol–gel method. The nitrates $Ce(NO_3)_3{\cdot}6H_2O$ and $Zr(NO_3)_4{\cdot}5H_2O$ were mixed according to the molar ratio of Ce:Zr = 67:33. Citric acid was used as the complexing agent. Appropriate glycol was added as the dispersant followed by evaporation and peptization. The sol was heated at 100 °C until a spongy yellow gel remained. Then the gel was submitted to decomposition at 300 °C for 1 h and calcination at 700 °C for 3 h. The synthesis process of Pt-doped ceria–zirconia solid solutions with the nominal molecular formula $Ce_{0.66}Zr_{0.32}Pt_{0.02}O_2$ was similar to that of $Ce_{0.67}Zr_{0.33}O_2$ powders except that the initial mixture consisted of $Ce(NO_3)_3{\cdot}6H_2O$, $Zr(NO_3)_4{\cdot}5H_2O$ and H_2PtCl_6 according to the molar ratio of Ce:Zr:Pt = 66:32:2. $Pt/Ce_{0.67}Zr_{0.33}O_2$ is prepared by impregnation method. The sol–gel-synthesized $Ce_{0.67}Zr_{0.33}O_2$ was mixed with the aqueous solution of H_2PtCl_6. The nominal loading of noble metal was 2 wt.%, which was equal to the amount of Pt in the Pt-doped sample. The mixture was stirred at 80 °C, dried at 110 °C and calcined at 500 °C for 3 h. Finally, the grayish powders were obtained as the Pt-loaded sample. An accelerating aging test was performed in a muffle furnace in static air at normal atmospheric pressure for a time period of 20 h at 950 °C.

2.2. Surface characterization

The X-ray diffraction analysis (XRD) was performed on a Japan Science D/max-RB diffractometer employing Cu Kα radiation (λ = 1.5418 Å). The X-ray tube was operated at 45 kV and 150 mA. The X-ray powder diffractogram was recorded at 0.02° intervals in the range $20° \leq 2\theta \leq 80°$ with 2 s count accumulation per step. The specific surface area was determined by Brunauer-Emmett-Teller (BET) method with a Quantachrome NOVA instrument using Ar as carrier and N_2 as adsorbent. The X-ray photoelectron spectroscopy (XPS) experiments were carried out on a PHI-5300 ESCA system with Al Kα radiation under UHV (1.33×10^{-8} Pa), calibrated internally by the carbon deposit C1s binding energy (BE) at 285 eV. Temperature-programmed reduction (TPR) experiments were carried out on a TPD/R/O 1100 catalytic surfaces analyzer. Typically 0.05 g of sample was employed. The standard pretreatment consisted of heating the powder sample in O_2 (5% in N_2, 30 ml min^{-1}) from room temperature to 600 °C (10 °C min^{-1}), holding at that temperature for 30 min, and then cooling down slowly, first in O_2/N_2 to 100 °C and finally to room temperature in He. After that, the samples were heated under flowing H_2 (5% in N_2, 20 ml min^{-1}) from room temperature to 1000 °C (10 °C min^{-1}).

2.3. Activity measurements

The powder catalyst sample was weighed for 1.0 g and mixed homogeneously with 6 ml coarse quartz particles.

The mixture was dried at 140 °C for 2 h, and then loaded in a quartz reaction tube with the diameter of 25 mm. The three-way catalytic activity was evaluated in a tube micro-reactor by passing a gas mixture simulated to exhaust from gasoline engine. The simulated exhaust contained a mixture of O_2 (1.5%), CO (1.5%), H_2 (0.5%), CO_2 (12%), C_3H_8 (0.1%), NO (0.05%) and N_2 (balance), corresponded to an oxidants/reductants stoichiometric factor $\lambda = (2O_2 + NO)/(CO + H_2 + 10C_3H_8)$ of 1.0. The concentrations of CO, C_3H_8 and NO were determined on-line by a five-component analyzer FGA4015 with infrared sensors. For the light-off experiments, the reactor was heated from 100 to 700 °C in the flow stream at a gas space velocity of 35,000 h^{-1}.

3. Results and discussion

3.1. XRD and BET studies

The X-ray diffraction patterns of $Ce_{0.67}Zr_{0.33}O_2$, Pt-doped and Pt-loaded samples before and after aging are shown in Fig. 1. The main peaks of the XRD patterns of all samples are consistent with the characteristic peaks of cubic CeO_2, which confirms the formation of ceria–zirconia solid solutions. The lattice constants of the ceria–zirconia-based materials are calculated based on Bragg's Law $2d\sin\theta = k\lambda$. Since the precision of the lattice parameter increases at higher diffraction angle, the peaks corresponding to the (3 1 1) crystallographic planes were chosen for calculation. For pure $Ce_{0.67}Zr_{0.33}O_2$, the fresh sample shows only the peaks due to a fluorite lattice structure pattern and the lattice constant is 0.5319 nm. After aging at 950 °C for 20 h, the weak peaks of the ZrO_2 phase ($2\theta = 30.24°$, intensity = 100; $2\theta = 50.30°$, intensity = 34; $2\theta = 59.28°$, intensity = 23) are found in the corresponding XRD pattern. Since the ionic radius of Zr^{4+} (0.84 Å) is smaller than that of Ce^{4+} (0.97 Å) for 8-coordination [17], the lattice constant of the cubic cell of ceria–zirconia solid solutions increases to 0.5343 nm as a result of the separation of the ZrO_2 or Zr-rich phase after aging.

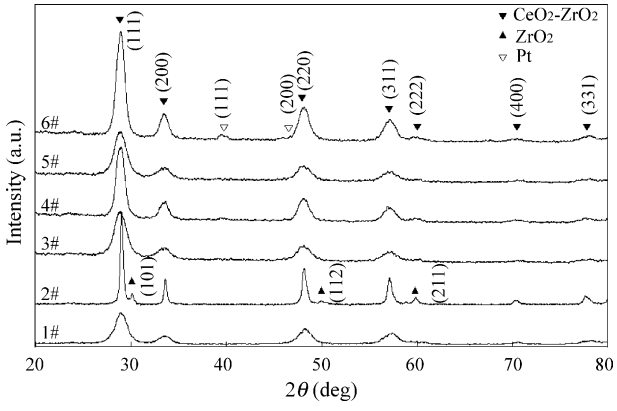

Fig. 1. XRD patterns of pure $Ce_{0.67}Zr_{33}O_2$ (fresh: 1#; aged: 2#), the Pt-doped (fresh: 3#; aged: 4#) and Pt-loaded (fresh: 5#; aged: 6#) samples.

No phase separation is observed for both the Pt-doped and Pt-loaded samples after aging. As reported in the literature [13], this strongly suggests the existence of a particular interaction between the noble metal and ceria. In this case, the presence of Pt seems to retard the demixing process in the $Ce_{0.67}Zr_{0.33}$ materials to form zirconia or Zr-rich phase. The ionic radius of Pt^{2+} is 0.80 Å and that of Pt^{4+} is 0.63 Å for 6-coordination, which are smaller than those of Zr^{4+} and Ce^{4+} [17]. Thus, it should cause a decrease of the value of the lattice parameter for indicating that the Pt^{2+} or Pt^{4+} ions have dissolved into the ceria lattice instead of the Zr^{4+} ions. Actually, the lattice constants for the fresh and aged Pt-doped samples are 0.5347 and 0.5349 nm, respectively, which are appreciably larger than that of $Ce_{0.67}Zr_{0.33}O_2$. The occurrence of this anomalous expansion implies a strong metal-support interaction (SMSI) between platinum and ceria–zirconia solid solutions, causing conversion of the Ce^{4+} (0.97 Å) to larger Ce^{3+} ions (1.14 Å for 8-coordination). The calculated lattice constants for the fresh and aged Pt-loaded samples were both 0.5346 nm, respectively, which also implies a similar SMSI effect.

No peaks of the platinum oxides (PtO or PtO_2) are observed in the XRD patterns of these Pt-containing samples since the main peaks of PtO_2 ($2\theta = 27.95°$, intensity = 100) and PtO ($2\theta = 33.90°$, intensity = 100) are quite close to two peaks of $Ce_{0.67}Zr_{0.33}O_2$ ($2\theta = 28.87°$, intensity = 100; $2\theta = 33.70°$, intensity = 35) and will be covered by them if there were. However, the weak peaks of metallic Pt^0 ($2\theta = 40.25°$, intensity = 100; $2\theta = 46.81°$, intensity = 45) are observed in the aged Pt-containing samples, especially in the aged Pt-loaded sample. This implies the decomposition of the Pt oxides and the agglomeration and growth of the Pt^0 crystallines after calcination at high temperature.

Compared with the fresh samples, the sharpening of the XRD patterns of the corresponding aged samples implies a significant sintering of the powders during calcination at high temperature. Accordingly, the BET surface area measured after aging decreases from an initial value of 57–11 m^2g^{-1} for the Pt-doped samples and from 41 to 10 m^2g^{-1} for the Pt-loaded samples. It is noted that, for the fresh samples, the surface area of the Pt-doped sample is larger than that of the Pt-loaded sample induced by an additional calcination step for the latter. After aging, the surface area of these two Pt-containing samples is quite similar.

3.2. XPS studies

It can be deduced from the result of XRD that the Pt ions have been partially introduced into the ceria lattice for the Pt-doped sample by sol–gel. For a further investigation, the X-ray photoelectron spectroscopy (XPS) experiment is performed to verify surface composition and elemental oxidation states.

Table 1
Surface elemental composition and atomic ratio of the Pt-containing samples measured by XPS

Sample	Surface composition (at.%)				Ce/Zr ratio	O/(Ce + Zr) Ratio	Pt/(Ce + Zr) ratio
	Pt	Ce	Zr	O			
Pt-doped, fresh (3#)	0.17	33.83	7.38	58.61	4.58	1.42	0.004
Pt-doped, aged (4#)	0.27	29.58	5.82	64.33	5.08	1.82	0.008
Pt-loaded, fresh (5#)	1.35	25.89	8.56	64.20	3.02	1.86	0.039
Pt-loaded, aged (6#)	0.53	26.58	6.97	65.91	3.81	1.96	0.016

The surface elemental composition of the Pt-doped and Pt-loaded samples calculated from the normalized peak areas of the Ce(3*d*), Pt(4*f*), Zr(3*d*) and O(1*s*) core level spectra is shown in Table 1. Using the values of surface atomic composition in Table 1, an estimation of the Ce/Zr and O/(Ce + Zr) atomic ratio can be obtained for the depth probed by XPS, which yields $Ce_{0.82}Zr_{0.18}O_{1.42}$, $Ce_{0.84}Zr_{0.16}O_{1.82}$, $Ce_{0.75}Zr_{0.25}O_{1.86}$ and $Ce_{0.79}Zr_{0.21}O_{1.96}$ for the samples 3–6#, respectively. It was proposed in the literature [18] that, during the hydrothermal aging at 1000 °C, the phase separation took place with surface enrichment in Zr, the Zr-rich phase being formed at the periphery of the particles, whereas the core was composed of the Ce-rich phase. In this case, the XPS analysis gives opposite information concerning the demixing mode. The surface Ce/Zr atomic ratio of these samples is much higher than the bulk Ce/Zr atomic ratio of 2.0, which means the outer part is rich in the cubic Ce-rich phase. On the other hand, it is observed that the surface oxygen concentration on these Pt-containing samples is lower than stoichiometric, indicating the existence of a significant amount of oxygen vacancies and cerium in the Ce^{3+} state. This also strongly proves an interaction between Pt and ceria–zirconia solid solutions, causing the reduction of the Ce^{4+} species. Especially for the Pt-doped samples, the relative higher value of the Ce/Zr atomic ratio and lower value of the O/(Ce + Zr) atomic ratio mean a stronger interaction between the dissolved Pt ions and ceria–zirconia solid solutions despite the lower surface Pt content. Compared with the bulk Pt/(Ce + Zr) ratio of 0.020, the surface Pt/(Ce + Zr) ratio calculated from the XPS signals is much lower for the fresh Pt-doped sample (0.004) and quite higher for the fresh Pt-loaded sample (0.039). This variation can be ascribed to different approaches of dispersing noble metal on ceria–zirconia solid solutions.

Pt 4*f* photoelectron spectra of the Pt-containing catalysts before and after aging are presented in Fig. 2. It is easy to see the effect of preparation methods and aging test on the spectra intensity. The intensity of the Pt 4*f* peaks for the Pt-doped samples decreases pronouncedly in comparison with the Pt-loaded samples due to the rather lower surface content of noble metal particles, which is confirmed by the decrease in the Pt/(Ce + Zr) ratio. The decreased intensity of the aged Pt-loaded sample may be attributed to sintering of Pt particles and structural changes in the ceria–zirconia support, such as loss of pore volume. However, this does not cause a decrease of the intensity of the aged Pt-doped sample. We suggest that the unaltered intensity may be induced by a contrary effect of the segregation of Pt out of the ceria lattice and dispersion as metallic Pt particles on the ceria–zirconia surface during the aging process, with the increase of surface composition of Pt and Pt/(Ce + Zr) serving as the evidence.

The measured Pt 4*f* spectra were peak-fitted with two components, one for metallic Pt and the other for Pt oxides. For example, the spectrum of the aged Pt-loaded sample (6#) gives two pairs of Pt $4f_{7/2}$ peak positions at 71.00 and 73.01 eV, both of which have a spin-orbit splitting of ca. 3.33 eV. According to Kaushik [19], the peaks for PtO should be at 72.4 and 75.6 eV while PtO_2 should show peaks at 74.1 and 77.4 eV. Thus, the Pt $4f_{7/2}$ peak position at 73.01 eV can be assigned to PtO (i.e. Pt^{2+}), but also PtO_2 (i.e. Pt^{4+}). It is observed that the fresh Pt-loaded sample (5#) mainly consist of Pt oxides, whereas the spectrum of the fresh Pt-doped sample presents in addition a new doublet at a lower binding energy. After aging, the spectra of both two Pt-containing samples present two doublets. Beside the interaction between Pt and oxygen, the formation of Pt oxides may be due to the existence of a Pt-Ce interaction as well [20–22]. Ceria is known for its ability to promote the oxidation of noble metals and their

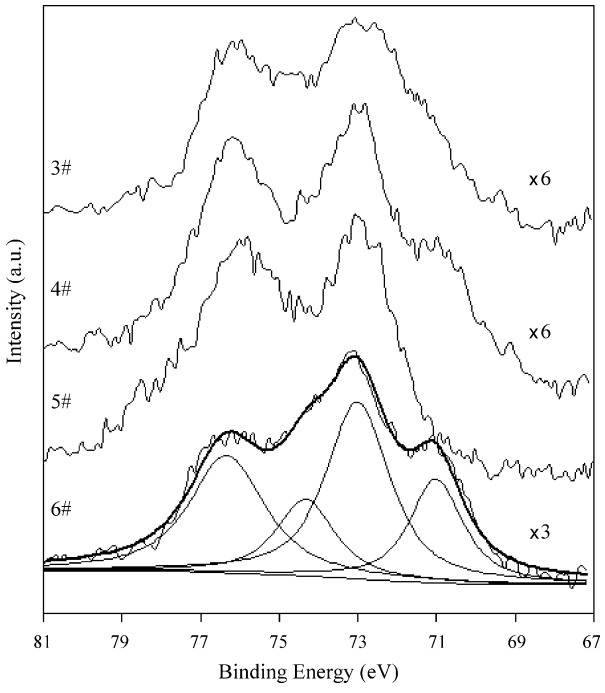

Fig. 2. Pt 4*f* spectra for the Pt-doped (fresh: 3#; aged: 4#) and Pt-loaded (fresh: 5#; aged: 6#) samples.

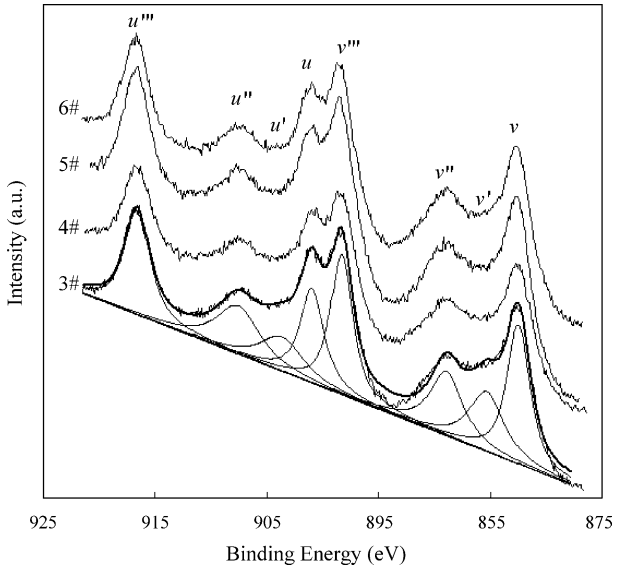

Fig. 3. Ce 3*d* spectra for the Pt-doped (fresh: 3#; aged: 4#) and Pt-loaded (fresh: 5#; aged: 6#) samples.

stabilization in an oxidized state because of the high redox potential of the Ce^{4+}/Ce^{3+} couple (1.61 eV), which is higher than those of the Pt^{2+}/Pt^{0} (1.19 eV) and Pt^{4+}/Pt^{2+} (1.05 eV) couples [17]. The oxidation of Pt may reflect charge transfer from metal to ceria, indicating that Ce is slightly reduced. This theory was supported by the fact that Pt promoted the reducibility of the surface ceria [23]. However, according to the area under each peak, there exists a proportion of 27 at.% Pt^{0} in the total Pt while scarcely metallic state for the fresh Pt-loaded sample, and the Pt^{0} contents in the total Pt are 39 and 34 at.% for the aged Pt-doped and Pt-loaded samples, respectively. Thus, a different synergistic effect between the platinum and cerium components in the Pt-doped sample is implied by the fact that more Pt oxides are reduced at 950 °C in an oxidative atmosphere compared with the Pt-loaded sample. The introduction of Pt into ceria–zirconia solid solutions appears to be capable of stabilizing Pt in a readily reducible form against the oxidizing effect of the Ce component and the calcination in air at high temperature for a long period.

The Ce 3*d* photoelectron spectra obtained from the samples 3–6# are shown in Fig. 3. It can be observed that each spectrum is composed by eight components. The peaks are assigned for Ce^{4+} as v, v'' and v''' for Ce $3d_{5/2}$, with the corresponding Ce $3d_{3/2}$ peaks labeled u, u'' and u'''. An additional doublet is also observed due to the presence of Ce^{3+} and is assigned v' and u'. Using the area under each peak, it is estimated that the fresh and aged Pt-doped samples are mostly non-stoichiometric with 78–82 at.% of the Ce 3*d* photoemission being due to Ce^{4+}, and the complement part, i.e. 22 down to 18 at.%, is ascribed to surface Ce^{3+}. For the Pt-loaded samples, the content of Ce^{3+} in the total Ce estimated from the XPS data is 19 and 16 at.% before and after aging, respectively. This is in good agreement with the surface atomic ratio of O/(Ce + Zr) in Table 1. The shift of the Ce^{3+} content in the aged samples is very likely due to the reduction of noble metal by the cerium component and/or the aging treatment in air. And the relative higher Ce^{3+} content in the Pt-doped sample probably suggests that incorporation of Pt into the ceria lattice may induce higher oxygen mobility in the bulk of ceria–zirconia solid solutions.

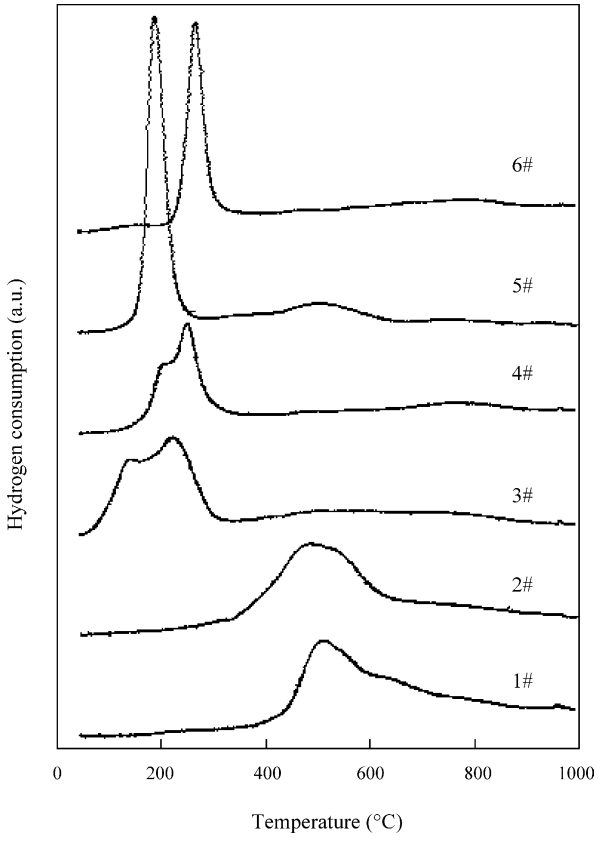

Fig. 4. TPR profiles of pure $Ce_{0.67}Zr_{33}O_2$ (fresh: 1#; aged: 2#), the Pt-doped (fresh: 3#; aged: 4#) and Pt-loaded (fresh: 5#; aged: 6#) samples.

3.3. TPR studies

The reducibility of all samples was determined by TPR and the results are shown in Fig. 4. The fresh $Ce_{0.67}Zr_{0.33}O_2$ solid solutions (1#) feature an intense peak at ca. 510 °C with a shoulder at ca. 580 °C. These two peaks are somehow overlapped. The reduction temperatures are considerably lower than that of CeO_2 (above 700 °C) [24], which is due to the increased mobility of bulk oxygen in ceria–zirconia solid solutions after the introduction of Zr^{4+} into the ceria lattice. After aging, the subsequent TPR profile features a doublet with one peak at ca. 470 °C and the other at ca. 540 °C (2#). The shift toward lower temperature for the reduction of the solid solution after aging is remarkable and strongly contrast what is usually observed for CeO_2 [5]. The total peak area of TPR profile for the aged $Ce_{0.67}Zr_{0.33}O_2$ is nearly unaltered in despite of its remarkably reduced surface area, which suggests the predominance of bulk reduction of the solid solutions.

The TPR profiles of the Pt-containing samples are significantly modified. It is noted that the peak at high temperature (450–550 °C) is dominant in the samples without Pt promotion, while the peak at low temperature (150–265 °C) is more prominent in the Pt-containing samples. For the fresh Pt-loaded sample (5#), only one peak is found at ca. 190 °C in the low temperature region, which is assigned to the combined reduction of Pt and Ce species with the main contribution from the Ce component. This indicates that the addition of noble metal effectively promotes the reduction of the $Ce_{0.67}Zr_{0.33}O_2$ support. It is attributed to the ability of the supported metal to active H_2 and then to spill it over onto the support [25]. In the absence of the metal, H_2 activation is difficult and may become the rate determining step. There is a very weak peak at ca. 510 °C in the high-temperature region, which may be assigned to the removal of surface oxygen from a very small percent of unpromoted ceria–zirconia powders. After aging, the peak attributed to the reduction of the Pt-promoted $Ce_{0.67}Zr_{0.33}O_2$ solid solution increases up to ca. 265 °C and the peak in the high-temperature region disappears. For the fresh Pt-doped sample, it can be seen that the reduction process splits into two peaks. A main peak at ca. 220 °C is supposed due to the combined reduction of part of Pt introduced into the ceria lattice and the Ce component, while a shoulder peak at ca. 150 °C can be attributed to the combined reduction of the surface Pt species and the Ce component. The shift towards lower temperature suggests that the reduction behavior of ceria–zirconia solid solutions can be further improved by introducing the Pt^{2+} ion into the ceria lattice, leading to higher oxygen mobility and easier bulk reduction of the solid solutions. After aging, the reduction temperature also increase, i.e. ca. 250 °C for the main peak and to ca. 205 °C for the shoulder. The smaller shift range of reduction temperature for the Pt-doped sample (30–55 °C) implies a better thermal stability than the Pt-loaded sample (75 °C).

3.4. Catalytic performance

In order to discuss the influence of preparation methods on the activity of the catalysts, the Pt-containing samples were evaluated as TWC under a stoichiometric simulated exhaust. Fig. 5a and b show the typical conversion curves for the three main pollutants – CO, C_3H_8 and NO – over the catalysts before and after an accelerating aging test, respectively. It can be seen that, in the low temperature domain, the fresh Pt-loaded sample (5#) by impregnation behaves a better three-way catalytic activity than that of the Pt-doped sample (3#) by sol–gel. It is mainly attributed to the promoting effect of the finely dispersed Pt crystallines on the high-surface-area ceria–zirconia solid solutions. It seems that the surface Pt species play a more important role in conversion of pollutants at low temperature than the bulk Pt species incorporated into the solid solutions since the Pt-doped sample shows an inferior catalytic performance. However, it is observed that both two catalysts reach the full conversion rates almost simultaneously and keep the same conversion curves at high temperature where is above 260 °C for CO, 300 °C for C_3H_8 and 480 °C for NO. This may be related to the synergistic effect between the Pt and Ce components in both two Pt–Ce–Zr–O systems via surface oxygen and bulk oxygen and still remains to be investigated.

After calcination at 950 °C for 20 h, the onsets of pollutant conversions are both retarded and the conversion curves are about the same. The advantage of the Pt-loaded sample (6#) disappears with the decrease of the surface Pt species and the thermal treatment strongly affects its catalytic activity. The T_{50} over the aged Pt-loaded sample shifts to high temperature with an increase of 105 °C for CO, 110 °C for C_3H_8 and 100 °C for NO. Whereas the increase of T_{50} over the Pt-doped sample (4#) is 55 °C for CO, 70 °C for C_3H_8 and 60 °C for NO, respectively. This suggests a better thermal stability for the Pt-doped sample to maintain an acceptable catalytic activity against high-temperature calcinations. It may be par-

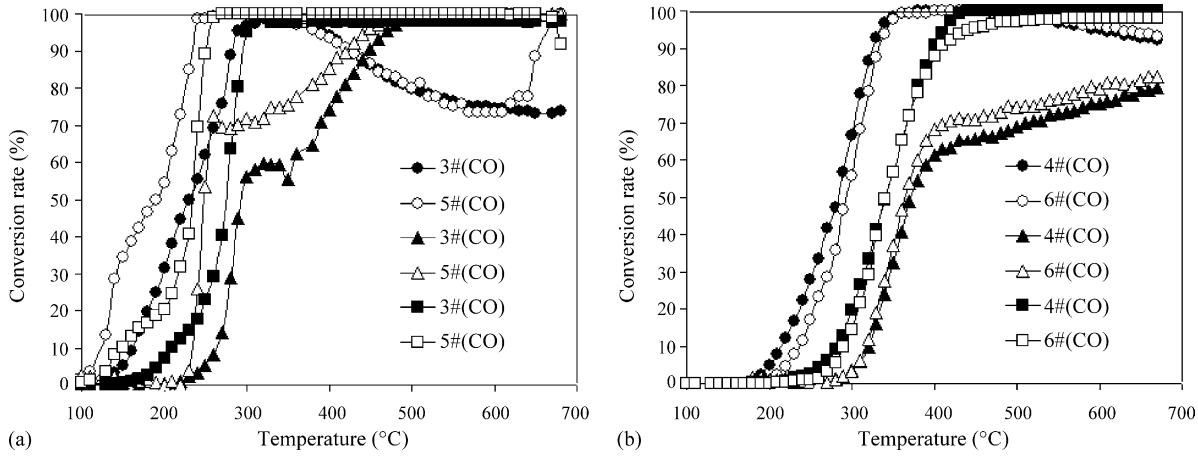

Fig. 5. Light-off curves of the fresh (a) and aged (b) catalysts, where 3#, 4# refer to Pt-doped samples and 5#, 6# refer to Pt-loaded samples.

tially attributed to the transformation of Pt from the bulk to the surface after calcination.

A so-called "self-regeneration" model has been presented that, in the noble metal doping perovskite-type oxides, the noble metal component occupies in the B-site of the perovskite structure under oxidizing atmosphere while it can segregates from the lattice and form the finely dispersed metallic particles on the crystal surface under reducing atmosphere [26–29]. In this case, a similar mechanism is supposed to exist in the Pt-doped ceria–zirconia solid solutions synthesized by sol–gel. It involves the complex conversion such as $Ce^{4+} + Pt \leftrightarrow Ce^{3+} + Pt^{2+}$ and oxygen-vacancy diffusion in the Pt–Ce–Zr–O system. It has been proved by the TPR result that the incorporation of Pt ions into the ceria lattice can promote the oxygen transfer and bulk reduction of the solid solutions. We have tried to construct a model to describe the influence of oxidative/reductive atmosphere on the structure and activity of this catalyst, and discussed the role of SMSI in the redox cycle [30]. However, many aspects of the proposed mechanism are still not understood.

4. Conclusions

We have known, based on the literatures, the universal preparation method of dispersing noble metal catalysts on ceria–zirconia solid solutions with alumina as carrier is wet-impregnation. In this study, a kind of Pt-doped ceria–zirconia solid solutions ($Ce_{0.66}Zr_{0.32}Pt_{0.02}O_2$) is synthesized by sol–gel in addition to a Pt-loaded catalyst (2 wt.% $Pt/Ce_{0.67}Zr_{0.33}O_2$) by impregnation. The results of XRD, XPS and TPR studies show that, through this method, part of Pt is introduced into the ceria lattice, potentially bringing about a different synergistic effect, such as higher oxygen mobility in ceria–zirconia solid solutions and larger reducibility of noble metal. After calcinations at 950 °C for 20 h, it shows a better thermal stability than the Pt-loaded one, implying a self-generation of noble metal in service.

Acknowledgements

The authors would like to acknowledge the Ministry of Science and Technology, PR China for the financial support of Project 2004CB719503, 2002AA643010 and 2004AA649400. Moreover, we would also thank the Center of Analysis in Tsinghua University for help with the XPS tests.

References

[1] T. Mikki, T. Ogawa, M. Haneda, N. Kakuta, A. Ueno, S. Tateishi, S. Matsuura, M. Sato, J. Phys. Chem. 94 (1990) 6464.
[2] B.K. Cho, J. Catal. 131 (1991) 74.
[3] T. Murota, T. Hasegawa, S. Aozasa, H. Matsui, M. Motoyama, J. Alloys Comp. 193 (1993) 298.
[4] M. Ozawa, M. Kimura, A. Isogai, J. Alloys Comp. 193 (1993) 73.
[5] P. Fornasiero, R. Dimonte, G. Ranga Rao, J. Kašpar, S. Meriani, A. Trovarelli, M. Graziani, J. Catal. 151 (1995) 168.
[6] A.E. Nelsona, K.H. Schulz, Appl. Surf. Sci. 210 (2003) 206.
[7] Y. Nagai, T. Yamamoto, T. Tanaka, S. Yoshida, T. Nonaka, T. Okamoto, A. Suda, M. Sugiura, Catal. Today 74 (2002) 225.
[8] S.S. Deshmukh, M.H. Zhang, V.I. Kovalchuk, J.L. d'Itri, Appl. Catal. B: Environ. 45 (2003) 135.
[9] G. Balducci, P. Fornasiero, R. Di Monte, J. Kašpar, S. Meriani, M. Graziani, Catal. Lett. 33 (1995) 193.
[10] G. Vlaic, R. Di Monte, P. Fornasiero, E. Fonda, J. Kašpar, M. Graziani, J. Catal. 182 (1999) 378.
[11] P. Fornasiero, E. Fonda, R. Di Monte, G. Vlaic, J. Kašpar, M. Graziani, J. Catal. 187 (1999) 177.
[12] K. Kenevey, F. Valdivieso, M. Soustelle, M. Pijolat, Appl. Catal. B: Environ. 29 (2001) 93.
[13] C. Bozo, N. Guilhaume, J.-M. Herrmann, J. Catal. 203 (2001) 393.
[14] M. Fernández-García, A. Martínez-Arias, A. Iglesias-Juez, A.B. Hungría, J.A. Anderson, J.C. Conesa, J. Soria, Appl. Catal. B: Environ. 31 (2001) 39.
[15] Y.Y. Liu, T. Hayakawa, T. Ishii, M. Kumagai, H. Yasuda, K. Suzuki, S. Hamakawa, K. Murata, Appl. Catal. A: Gen. 210 (2001) 301.
[16] A. Primavera, A. Trovarrelli, C. De Leitenburg, G. Dolcetti, J. Llorca, Stud. Surf. Sci. Catal. 199 (1998) 87.
[17] J.A. Dean, Lange's Handbook of Chemistry, 15th ed., McGraw-Hill, New York, 1998.
[18] C. Bozo, F. Gaillard, N. Guilhaume, Appl. Catal. A: Gen. 220 (2001) 75.
[19] V.K. Kaushik, Z. Phys. Chem. 173 (1991) 105.
[20] L. Olsson, E. Fridell, J. Catal. 210 (2002) 348.
[21] M.J. Tiernan, O.E. Finlayson, Appl. Catal. B: Environ. 19 (1998) 27.
[22] A. Trovarelli, Catal. Rev. Sci. Eng. 38 (1996) 439.
[23] C. Serre, F. Garin, G. Belot, G. Maire, J. Catal. 141 (1993) 1.
[24] F.B. Noronha, E.C. Fendlei, R.R. Soares, W.E. Alvarez, D.E. Resasco, Chem. Eng. J. 82 (2001) 28.
[25] M.F. Luo, X.M. Zheng, Appl. Catal. A: Gen. 189 (1999) 19.
[26] Y. Nishihata, J. Mizuki, T. Akao, H. Tanaka, M. Uenishi, M. Kimura, T. Okamoto, N. Hamada, Nature 148 (2002) 164.
[27] N. Guilhaume, M. Primet, J. Catal. 165 (1997) 197.
[28] H. He, H.X. Dai, C.T. Au, Appl. Catal. B: Environ. 33 (2001) 65.
[29] H. Tanaka, M. Misono, Curr. Opin. Solid State Mat. Sci. 5 (2001) 381.
[30] J. Fan, X.D. Wu, R. Ran, D. Weng, Appl. Surf. Sci. (2005), accepted.